A Push-Button Molecular Switch

Jason M. Spruell,[†] Walter F. Paxton,[†] John-Carl Olsen,[†] Diego Benítez,[‡]
Ekaterina Tkatchouk,[‡] Charlotte L. Stern,[†] Ali Trabolsi,[†] Douglas C. Friedman,[†]
William A. Goddard III,[‡] and J. Fraser Stoddart*[,†]

*Department of Chemistry, Northwestern University, 2145 Sheridan Road, Evanston,
Illinois 60202, and Materials and Process Simulation Center, California Institute of Technology,
Pasadena, California 91125*

Received May 20, 2009; E-mail: stoddart@northwestern.edu

Abstract: The preparation, characterization, and switching mechanism of a unique single-station mechanically switchable hetero[2]catenane are reported. The facile synthesis utilizing a "threading-followed-by-clipping" protocol features Cu^{2+}-catalyzed Eglinton coupling as a mild and efficient route to the tetrathiafulvalene-based catenane in high yield. The resulting mechanically interlocked molecule operates as a perfect molecular switch, most readily described as a "push-button" switch, whereby two discrete and fully occupied translational states are toggled electrochemically at incredibly high rates. This mechanical switching was probed using a wide variety of experimental techniques as well as quantum-mechanical investigations. The fundamental distinctions between this single-station [2]catenane and other more traditional bi- and multistation molecular switches are significant.

Introduction

The chemistry of catenanes[1] has experienced a resurgence in recent years, driven in part by improved template-directed protocols[2] enabling their synthesis as well as technical applications made possible by virtue of their unique molecular topologies. Through the use of molecular recognition and self-assembly,[1a,c,3] mechanically interlocked molecules (MIMs) have been efficiently created, allowing the use of these chemical

compounds as the basis for constructing artificial molecular machines[4] and fabricating molecular electronic devices.[5] The introduction of bi- and multistable MIM platforms[5a,c,6] enables

[†] Northwestern University.
[‡] California Institute of Technology.

(1) (a) Schalley, C. A.; Weilandt, T.; Brüggemann, J.; Vögtle, F. *Top. Curr. Chem.* **2004**, *248*, 141–200. (b) Godt, A. *Eur. J. Org. Chem.* **2004**, 1639–1654. (c) Collin, J.-P.; Heitz, V.; Sauvage, J.-P. *Top. Curr. Chem.* **2005**, *262*, 29–62. (d) Lankshear, M. D.; Beer, P. D. *Acc. Chem. Res.* **2007**, *40*, 657–668. (e) Dichtel, W. R.; Miljanić, O. Š.; Zhang, W.; Spruell, J. M.; Patel, K.; Aprahamian, I.; Heath, J. R.; Stoddart, J. F. *Acc. Chem. Res.* **2008**, *41*, 1750–1761. (f) Fujita, M. *Acc. Chem. Res.* **1999**, *32*, 53–61.
(2) (a) Busch, D. H.; Stephenson, N. A. *Coord. Chem. Rev.* **1999**, *100*, 139–154. (b) Anderson, S.; Sanders, J. K. M. *Acc. Chem. Res.* **1993**, *26*, 469–475. (c) Cacciapaglia, R.; Mandolini, L. *Chem. Soc. Rev.* **1993**, *22*, 221–231. (d) Hoss, R.; Vögtle, F. *Angew. Chem., Int. Ed. Engl.* **1994**, *33*, 374–384. (e) Schneider, J. P.; Kelly, J. W. *Chem. Rev.* **1995**, *95*, 2169–2187. (f) Raymo, F. M.; Stoddart, J. F. *Pure Appl. Chem.* **1996**, *68*, 313–322. (g) *Templated Organic Synthesis*; Diederich, F., Stang, P. J., Eds.; Wiley-VCH: Weinheim, Germany, 1999. (h) Stoddart, J. F.; Tseng, H.-R. *Proc. Natl. Acad. Sci. U.S.A.* **2002**, *99*, 4797–4800. (i) Aricó, F.; Badjić, J. D.; Cantrill, S. J.; Flood, A. H.; Leung, K. C.-F.; Liu, Y.; Stoddart, J. F. *Top. Curr. Chem.* **2005**, *249*, 203–259. (j) Williams, A. R.; Northrop, B. H.; Chang, T.; Stoddart, J. F.; White, A. J. P.; Williams, D. J. *Angew. Chem., Int. Ed.* **2006**, *45*, 6665–6669. (k) Northrop, B. H.; Aricó, F.; Tangchiavang, N.; Badjić, J. D.; Stoddart, J. F. *Org. Lett.* **2006**, *8*, 3899–3902. (l) Cantrill, S. J.; Poulin-Kerstein, K. G.; Grubbs, R. H.; Lanari, D.; Leung, K. C.-F.; Nelson, A.; Smidt, S. P.; Stoddart, J. F.; Tirrell, D. A. *Org. Lett.* **2005**, *7*, 4213–4216.
(3) (a) *Molecular Catenanes, Rotaxanes, and Knots*; Sauvauge, J.-P., Dietrich-Buchecker, C., Eds.; Wiley-VCH: Weinheim, Germany, 1999. (b) Philp, D.; Stoddart, J. F. *Angew. Chem., Int. Ed. Engl.* **1996**, *35*, 1154–1156. (c) Philp, D.; Stoddart, J. F. *Synlett* **1991**, 445–458.

(4) (a) Balzani, V.; Credi, A.; Venturi, M. *Molecular Devices and Machines: A Journey into the Nano World*; Wiley-VCH: Weinheim, Germany, 2008. (b) Kay, E. R.; Leigh, D. A.; Zerbetto, F. *Angew. Chem., Int. Ed.* **2007**, *46*, 71–191. (c) Serreli, V.; Lee, C.-F.; Kay, E. R.; Leigh, D. A. *Nature* **2007**, *445*, 523–527. (d) Saha, S.; Stoddart, J. F. *Chem. Soc. Rev.* **2007**, 77–92.
(5) (a) Luo, Y.; Collier, C. P.; Jeppesen, J. O.; Nielsen, K. A.; DeIonno, E.; Ho, G.; Perkins, J.; Tseng, H.-R.; Yamamoto, T.; Stoddart, J. F.; Heath, J. R. *ChemPhysChem* **2002**, *3*, 519–525. (b) Tseng, H.-R.; Nu, D.; Fang, N. X.; Zhang, X.; Stoddart, J. F. *ChemPhysChem* **2004**, *5*, 111–116. (c) Flood, A. H.; Stoddart, J. F.; Steuerman, D. W.; Heath, J. R. *Science* **2004**, *306*, 2055–2056. (d) Beckman, R.; Beverly, K.; Boukai, A.; Bunimovich, Y.; Choi, J. W.; DeIonno, E.; Green, J.; Johnston-Halperin, E.; Luo, Y.; Sheriff, B.; Stoddart, J. F.; Heath, J. R. *Faraday Discuss.* **2006**, *131*, 9–22. (e) Green, J. E.; Choi, J. W.; Boukai, A.; Bunimovich, Y.; Johnston-Halperin, E.; DeIonno, E.; Luo, Y.; Sheriff, B. A.; Xu, K.; Shin, Y. S.; Tseng, H.-R.; Stoddart, J. F.; Heath, J. R. *Nature* **2007**, *445*, 414–417. (f) Ball, P. *Nature* **2007**, *445*, 362–363. (g) Dichtel, W. R.; Heath, J. R.; Stoddart, J. F. *Philos. Trans. R. Soc. London, Ser. A* **2007**, *365*, 1605–1625.
(6) (a) Liu, Y.; Flood, A. H.; Bonvallet, P. A.; Vignon, S. A.; Tseng, H.-R.; Huang, T. J.; Brough, B.; Baller, M.; Magonov, S.; Solares, S.; Goddard, W. A., III; Ho, C.-M.; Stoddart, J. F. *J. Am. Chem. Soc.* **2005**, *127*, 9745–9759. (b) Balzani, V.; Credi, A.; Ferrer, B.; Silvi, S.; Venturi, M. *Top. Curr. Chem.* **2005**, *262*, 1–27. (c) Mandl, C. P.; König, B. *Angew. Chem., Int. Ed.* **2004**, *43*, 1622–1624. (d) Hernández, J. V.; Kay, E. R.; Leigh, D. A. *Science* **2004**, *306*, 1532–1537. (e) Leigh, D. A.; Wong, J. K. Y.; Dehez, F.; Zerbetto, F. *Nature* **2003**, *424*, 174–179. (f) *Molecular Switches*; Feringa, B. L., Ed.; Wiley-VCH: Weinheim, Germany, 2001. (g) Flood, A. H.; Peters, A. J.; Vignon, S. A.; Steuerman, D. W.; Tseng, H.-R.; Kang, S.; Heath, J. R.; Stoddart, J. F. *Chem.—Eur. J.* **2004**, *10*, 6558–6564. (h) Steuerman, D. W.; Tseng, H.-R.; Peters, A. J.; Flood, A. H.; Jeppesen, J. O.; Nielsen, K. A.; Stoddart, J. F.; Heath, J. R. *Angew. Chem., Int. Ed.* **2004**, *43*, 6486–6491. (i) Tseng, H.-R.; Vignon, S. A.; Celestre, P. C.; Perkins, J.; Jeppesen, J. O.; Di Fabio, A.; Ballardini, R.; Gandolfi, M. T.; Venturi, M.; Balzani, V.; Stoddart, J. F. *Chem.—Eur. J.* **2004**, *10*, 155–172.

these applications, particularly if the basis for switching involves electrochemical processes.

Our long-standing interest in the synthesis and applications of charged MIMs, specifically those that incorporate as one ring component the π-electron-poor tetracationic cyclophane cyclobis(paraquat-*p*-phenylene) (CBPQT[4+]),[7] has led to the production of a variety of electrochemically switchable molecules.[5,8] Traditionally, CBPQT[4+]-based catenanes and rotaxanes have been synthesized by "clipping" a partially formed CBPQT[4+] ring around a π-donor unit[9] [e.g., 1,5-dioxynaphthalene (DNP) or tetrathiafulvalene (TTF)] as part of a preformed macrocycle or a dumbbell compound. While this approach has successfully yielded a number of useful compounds in the past, recent investigations[1e,10,11] have shown that the synthesis of MIMs from pseudorotaxanes containing fully formed CBPQT[4+] rings can be more effective and efficient. Central to the implementation of this "threading-followed-by-clipping" approach to catenane synthesis has been the introduction of ultramild reactions to effect the final macrocyclization, yielding the catenane in the presence of the CBPQT[4+] ring, which is sensitive to bases, nucleophiles, and reducing agents. Of particular success has been the use of Cu^{+}- and Cu^{2+}-mediated processes in alkyne-based couplings, such as the CuAAC reaction[12] and Eglinton coupling.[13]

Here we report (*i*) the facile template-directed synthesis and characterization of a switchable [2]catenane through Cu^{2+}-mediated Eglinton coupling[13] on a [2]pseudorotaxane formed between CBPQT[4+] and a bispropargyl-functionalized TTF unit; since this [2]catenane contains a single switchable binding station, (*ii*) it exists in one translational form in its ground state that (*iii*) may be mechanically switched wholly to another translational form in the excited oxidized state and (*iv*) exhibits very fast and reversible switching between the two forms. Moreover, this compound expands our understanding of the mechanics of switching within a catenated framework whereby the elimination of the weaker secondary binding station
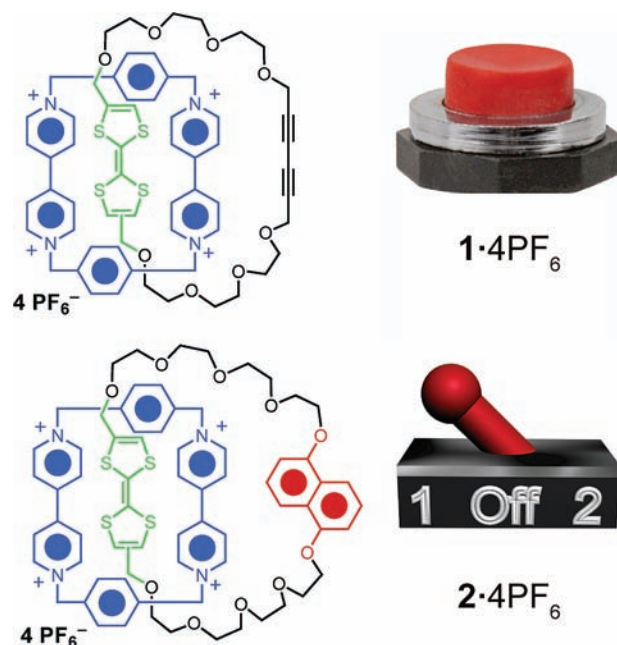

Figure 1. Structural formulas of (top) the switchable single-station [2]catenane **1**·4PF₆, which is represented as a two-state push-button molecular switch incorporating a single tetrathiafulvalene (TTF) station, and (bottom) the traditional switchable bistable [2]catenane **2**·4PF₆, which is represented as a three-state switch incorporating both TTF and 1,5-dioxynaphthalene (DNP) stations.

traditionally found in bistable MIMs results in the reduction of complexity to that of a simple push-button-operated switch (Figure 1). In the parlance[14] of electrical engineering, this "single-pole single-throw" (SPST) molecular switch operates between two distinct working positions through electrochemical stimuli. The simplicity of this single-station switch stands in contrast to previously constructed,[5] more complicated bi- and multistation molecular switches analogous to "single-pole double-throw" (SPDT) switches. These observations and perspectives are supported by a solid-state structure, extensive NMR spectroscopic studies, cyclic voltammetry, and spectroelectrochemistry as well as computational investigations.

Results and Discussion

Variants of Eglinton coupling have been used extensively to prepare [2]- and [3]catenanes of mixed compositions through both covalent-[1b,15] and template-directed[16] protocols. We recently applied[11] this useful homocoupling to prepare hetero[2]-catenanes bearing DNP as a single station for a CBPQT[4+] ring in very high yields under mild conditions. Inspired by the novelty of these simple, high-yield approaches to catenane synthesis, we speculated that the same protocols could be

(7) (a) Doddi, G.; Ercolani, G.; Mencarelli, P.; Piermattei, A. *J. Org. Chem.* **2005**, *70*, 3761–3764. (b) Asakawa, M.; Dehaen, W.; L'abbé, G.; Menzer, S.; Nouwen, J.; Raymo, F. M.; Stoddart, J. F.; Williams, D. J. *J. Org. Chem.* **1996**, *61*, 9591–9595. (c) Odell, B.; Reddington, M. V.; Slawin, A. M. Z.; Spencer, N.; Stoddart, J. F.; Williams, D. J. *Angew. Chem., Int. Ed. Engl.* **1988**, *27*, 1547–1550.

(8) Asakawa, M.; Ashton, P. R.; Balzani, V.; Credi, A.; Hamers, C.; Mattersteig, G.; Montalti, M.; Shipway, A. N.; Spencer, N.; Stoddart, J. F.; Tolley, M. S.; Venturi, M.; White, A. J. P.; Williams, D. J. *Angew. Chem., Int. Ed.* **1998**, *37*, 333–337.

(9) (a) Ashton, P. R.; Goodnow, T. T.; Kaifer, A. E.; Reddington, M. V.; Slawin, A. M. Z.; Spencer, N.; Stoddart, J. F.; Vicent, C.; Williams, D. J. *Angew. Chem., Int. Ed. Engl.* **1989**, *28*, 1396–1399. (b) Anelli, P.-L.; Spencer, N.; Stoddart, J. F. *J. Am. Chem. Soc.* **1991**, *113*, 5131–5133.

(10) (a) Dichtel, W. R.; Miljanić, O. Š.; Spruell, J. M.; Heath, J. R.; Stoddart, J. F. *J. Am. Chem. Soc.* **2006**, *128*, 10388–10390. (b) Braunschweig, A. B.; Dichtel, W. R.; Miljanić, O. Š.; Olson, M. A.; Spruell, J. M.; Khan, S. I.; Heath, J. R.; Stoddart, J. F. *Chem.—Asian J.* **2007**, *2*, 634–647. (c) Miljanić, O. Š.; Dichtel, W. R.; Aprahamian, I.; Rohde, R. D.; Agnew, H. D.; Heath, J. R.; Stoddart, J. F. *QSAR Comb. Sci.* **2007**, *26*, 1165–1174. (d) Spruell, J. M.; Dichtel, W. R.; Heath, J. R.; Stoddart, J. F. *Chem.—Eur. J.* **2008**, *14*, 4168–4177.

(11) (a) Miljanić, O. Š.; Dichtel, W. R.; Mortezaei, S.; Stoddart, J. F. *Org. Lett.* **2006**, *8*, 4835–4838. (b) Miljanić, O. Š.; Dichtel, W. R.; Khan, S. I.; Mortezaei, S.; Heath, J. R.; Stoddart, J. F. *J. Am. Chem. Soc.* **2007**, *129*, 8236–8246.

(12) For Cu-catalyzed azide–alkyne cycloaddition, see: Rostovtsev, V. V.; Green, L. G.; Fokin, V. V.; Sharpless, K. B. *Angew. Chem., Int. Ed.* **2002**, *41*, 2596–2599.

(13) For a comprehensive review of Glaser, Eglinton, and related alkyne couplings, see: (a) Siemsen, P.; Livingston, R. C.; Diederich, F. *Angew. Chem., Int. Ed.* **2000**, *39*, 2632–2657. For the original report, see: (b) Eglinton, G.; Galbraith, A. R. *Chem. Ind. (London)* **1956**, 737–738.

(14) Kim, H. C.; Chun, K. *IEEJ Trans.* **2007**, *2*, 249–261.

(15) (a) Duda, S.; Godt, A. *Eur. J. Org. Chem.* **2003**, 3412–3420. (b) Ünsal, Ö.; Godt, A. *Chem.—Eur. J.* **1999**, *5*, 1728–1733.

(16) (a) Hamilton, D. G.; Sanders, J. K. M.; Davies, J. E.; Clégg, W.; Teat, S. J. *Chem. Commun.* **1997**, 897–898. (b) Hamilton, D. G.; Feeder, N.; Prodi, L.; Teat, S. J.; Clégg, W.; Sanders, J. K. M. *J. Am. Chem. Soc.* **1998**, *120*, 1096–1097. (c) Hamilton, D. G.; Prodi, L.; Feeder, N.; Sanders, J. K. M. *J. Chem. Soc., Perkin Trans. 1* **1999**, 1057–1065. (d) Dietrich-Buchecker, C. O.; Hemmert, C.; Khémiss, A.-K.; Sauvage, J.-P. *J. Am. Chem. Soc.* **1990**, *112*, 8002–8008. (e) Dietrich-Buchecker, C. O.; Khémiss, A.; Sauvage, J.-P. *J. Chem. Soc., Chem. Commun.* **1986**, 1376–1378. (f) Gunter, M. J.; Farquhar, S. M. *Org. Biomol. Chem.* **2003**, *1*, 3450–3457. (g) Sato, Y.; Yamasaki, R.; Saito, S. *Angew. Chem., Int. Ed.* **2009**, *48*, 504–507.
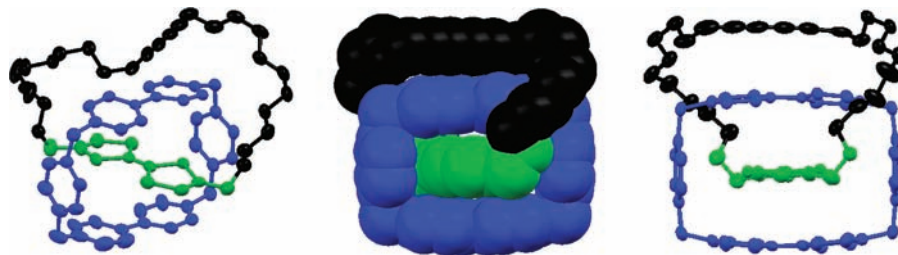
Figure 2. Solid-state structure of 1^{4+} displayed from two angles. The disordered PF_6^- counterions, hydrogen atoms, and solvent molecules have been omitted for clarity. The $CBPQT^{4+}$ ring is shown in blue, the TTF unit in green, and the butadiyne and glycol units in black.

employed to create a hetero[2]catenane bearing the electrochemically switchable TTF unit and thus arrive at an electrochemically switchable catenane.

TTF and its derivatives have been used extensively[5,8] to create electrochemically switchable MIMs. The π-electron-rich neutral state may be reversibly oxidized either once or twice to π-electron-poor radical cation and dication states, respectively. Toggling between the neutral and oxidized states when the TTF is incorporated into a catenane or rotaxane containing $CBPQT^{4+}$ allows the ejection of the oxidized TTF^{2+} dication from inside the ring through electrostatic repulsion. Usually, a weaker secondary binding station, such as DNP, is incorporated into the molecule to replace the oxidized TTF^{2+} dication within the $CBPQT^{4+}$ cavity upon its ejection, providing a discrete, long-lived switched co-conformation even following the reinstatement of the neutral TTF unit. Breaking with this tradition, we synthesized a single-station [2]catenane, compound $1 \cdot 4PF_6$, that operates through an electrostatic-repulsion mechanism and may be switched between two discrete translational states (see below), eliminating the need for a secondary station.

The π-electron-rich TTF derivative **4** was prepared by propargylation of the two arms of TTF diol **3** (Scheme 1).[17] When **4** and $CBPQT \cdot 4PF_6$ were mixed in a 2:1 molar ratio[18] in MeCN, the solution became an intense emerald-green as a consequence of the formation of pseudorotaxane $[4 \subset CBPQT] \cdot 4PF_6$. Reaction with $Cu(OAc)_2 \cdot H_2O$ (1.25 equiv per terminal alkyne) at 23 °C for 2 days effected the desired Eglinton coupling, affording the [2]catenane $1 \cdot 4PF_6$ as a green solid in 64% yield. This exceptionally high yield in the formation of a complex, mechanically interlocked topology through macrocyclization reflects the synthetic advantages of the "threading-followed-by-clipping" approach invoked in its design. A very similar [2]catenane, $2 \cdot 4PF_6$ (Figure 1), containing both TTF and DNP recognition units was prepared previously[8] by the traditional "clipping" of a partially formed $CBPQT^{4+}$ ring around one of these recognition sites in the TTF/DNP macrocycle. Although this protocol produced a very useful bistable molecular switch, the final "clipping" step afforded that catenane in only 23% yield. The current method affords a switchable catenane in much higher yield than that previously reported, and the structural replacement of the DNP binding moiety with the butadiyne unit in compound $1 \cdot 4PF_6$ affects the switching behavior of the molecule profoundly.

Slow diffusion of iPr_2O into a MeCN solution of $1 \cdot 4PF_6$ at room temperature produced light-green needlelike single crystals

Scheme 1
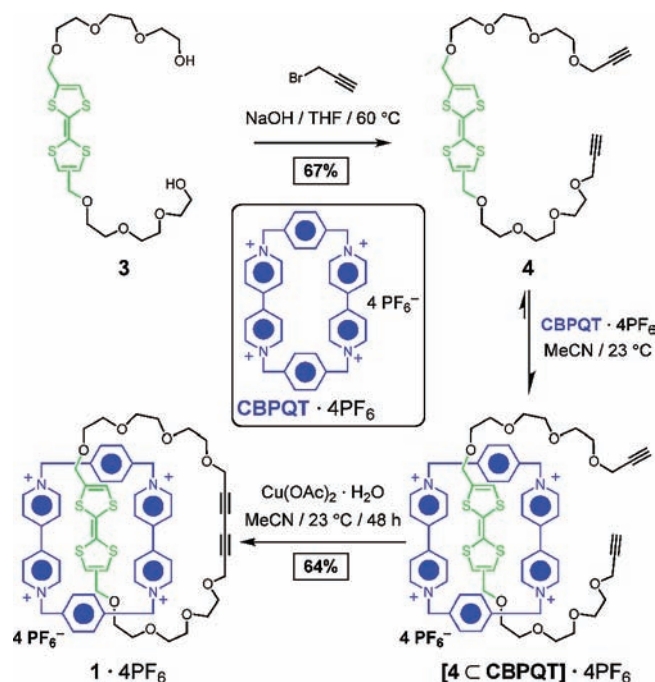
suitable for X-ray structural analysis.[19] Two different views of the solid-state structure of 1^{4+}, represented either as ellipsoids or with a space-filling representation, are shown in Figure 2. Of the two constitutional isomers possible for disubstituted TTF, only the trans isomer was observed in the solid state, as in the case of the previously reported[8] TTF/DNP catenane. The $CBPQT^{4+}$ ring encircles the TTF unit in an association that is stabilized through a combination of π–π stacking interactions[20] and [C–H···O] interactions from α-bipyridinium hydrogen atoms to, in one instance, the second and third oxygen atoms away from the TTF in the oligoether chain and, in another, to the second oxygen atom away from the TTF in the oligoether chain.[21] In common with the previously reported[11b] DNP-based Eglinton-coupled catenanes, the butadiyne fragment is aligned approximately parallel to the external bipyridinium face of the

(17) Compound **3** was synthesized using a procedure slightly modified from that given in the following reference: Tseng, H.-R.; Vignon, S. A.; Celestre, P. C.; Perkins, J.; Jeppesen, J. O.; Fabio, A. D.; Ballardini, R.; Gandolfi, M. T.; Venturi, M.; Balzani, V.; Stoddart, J. F. *Chem.–Eur. J.* **2004**, *10*, 155–172.

(18) $CBPQT \cdot 4PF_6$ was used as the limiting reagent to ensure the full conversion of all charged material to [2]catenane $1 \cdot 4PF_6$, facilitating its purification as the sole charged component in an assortment of organic products derived from Eglinton coupling of **4**.

(19) Crystal description: $C_{79.50}H_{93}F_{24}N_{12.50}O_8P_4S_4$; $M_r = 2059.78$; triclinic; space group $P\bar{1}$; $a = 14.0138(4)$ Å, $b = 14.0734(2)$ Å, $c = 25.1493(5)$ Å, $\alpha = 98.2070(10)°$, $\beta = 105.1000(10)°$, $\gamma = 91.9490(10)°$; $V = 4726.5(2)$ Å^3; $Z = 2$; $T = 100(2)$ K; 65124 reflections collected, 16991 independent reflections ($R_{int} = 0.0375$); $R(F) = 0.0979$, $wR_2 = 0.2687$. Disordered MeCN molecules as well as PF_6^- counterions are also present within the structure.

(20) A mean π–π distance of 3.35 Å between the bipyridinium faces and the encircled TTF unit was observed.

(21) [C–H···O] short contacts of 2.41, 2.54, and 2.34 Å with corresponding angles of 166.7, 117.24, and 169.06° were measured for the second, third, and second oxygens away from the TTF unit, respectively.
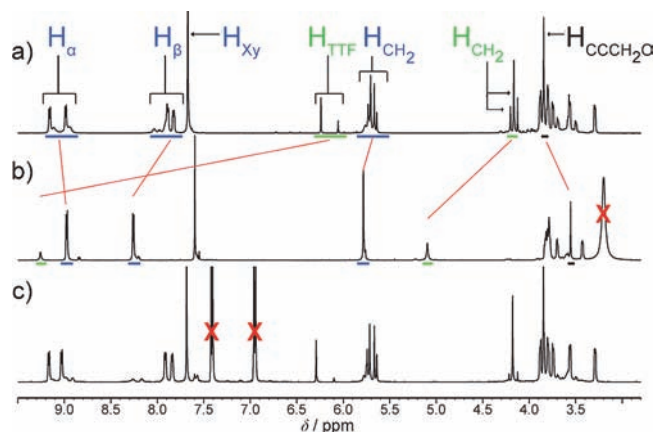
Figure 3. ^{1}H NMR spectra (500 MHz, CD$_3$CN, 293 K) of (a) compound **1**·4PF$_6$, (b) fully oxidized **1**[6+] after the addition of 2 equiv of the chemical oxidant tris(4-bromophenyl)ammoniumyl hexachloroantimonate, and (c) rereduced **1**[4+] after the addition of Zn dust. Resonances due to the chemical oxidant and residual solvent are marked with red "X" symbols.

CBPQT[4+] cyclophane with an interplanar distance of 3.34 Å, a short contact that could be a consequence of a stabilizing $\pi-\pi$ interaction. In the presence of its four disordered PF$_6^-$ counterions, catenane **1**[4+] packs with the butadiyne units as the closest point of contact and so does not form an extended donor–acceptor stacking arrangement.

^{1}H NMR spectroscopy (Figure 3a) provides additional confirmation of the interlocked nature of **1**·4PF$_6$ as well as the relative position of the CBPQT[4+] ring encircling the TTF unit exclusively in the ground state. Most notable is the presence of two sets of signals arising from both the α- and β-bipyridinium protons of the CBPQT[4+] ring at room temperature. When the CBPQT[4+] ring encircles the TTF moiety, the local symmetry of the TTF unit is commuted to the CBPQT[4+] ring, rendering the pairs of α- and β-bipyridinium protons heterotopic and thus separating each into a set of anisochronous signals.[22] Interestingly, although the cis and trans isomers of the disubstituted TTF unit can rapidly interconvert[23] in the presence of a trace of acid, both configurational isomers appear to be present after isolation and purification of **1**·4PF$_6$. Two clear singlets corresponding to the protons on the TTF rings are observed at 6.24 and 6.06 ppm in a 3:1 ratio. This ratio is repeated throughout the entire spectrum, not only for the signals of protons neighboring the TTF and ethylene glycol units of its own macrocycle but also for those of the CBPQT[4+] ring. Upon chemical oxidation and subsequent reduction of the TTF that effects the translational switching of the catenane (see below), this ratio increases to 13:1 in favor of the major (most likely trans) configurational isomer. Interestingly, this same distribution is obtained without switching of the molecule after the catenane has remained in solution for at least 5 months, indicating that this distribution represents the equilibrium state of the configu-

rational isomers within this catenane. We believe that this equilibrium is reached so much more slowly here than in other TTF-based mechanically interlocked systems because, in this unique catenane, TTF constitutes the only station for the CBPQT[4+] ring. In bistable systems, such as **2**·4PF$_6$, the CBPQT[4+] ring is commonly distributed between the two stations within the ensemble to a degree that depends on the relative binding affinities of the constituents, so for a single molecule, although the CBPQT[4+] ring sits around the TTF unit more often than the competing station on average, it spends a considerable amount of time well away from the TTF unit. We propose that it is only during this "off time" that the TTF is able to interconvert between its cis and trans configurational isomers. Since there is minimal "off time" in the case of the single-station catenane **1**[4+], the CBPQT[4+] ring kinetically traps the TTF, increasing the time necessary for it to equilibrate into its steady-state distribution of configurational isomers.

Scheme 2
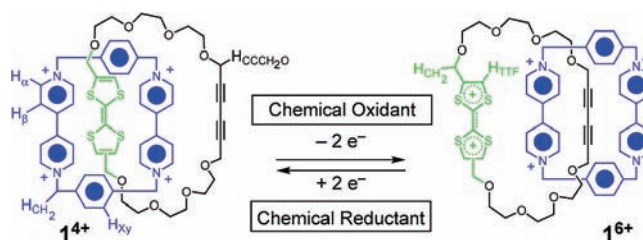
Chemical oxidation of **1**[4+] to **1**[6+] (Scheme 2) was performed in CD$_3$CN using 2 equiv of tris(4-bromophenyl)ammoniumyl hexachloroantimonate as the chemical oxidant,[24] and the effects of chemical switching were probed using ^{1}H NMR spectroscopy. After oxidation, substantial changes were observed in the ^{1}H NMR spectrum (Figure 3b). Most notable were the large downfield shifts for the resonances corresponding to the TTF[2+] protons as well as those for the methylene protons neighboring the TTF[2+] dication. Such large shifts are a consequence of the buildup of positive charge, which is shared across the TTF unit. Structurally, this oxidation forces the tetracationic CBPQT[4+] ring away from the TTF[2+] unit, moving it to the position furthest away. The relationship between the TTF and butadiyne units within their macrocycle dictates that the butadiyne unit represents the position furthest away from the TTF[2+] unit and the most stable site for the CBPQT[4+] ring in **1**[6+]. The resonances for the methylene units neighboring the butadiyne were shifted upfield by 0.29 ppm, reflecting the movement of the encircling CBPQT[4+] ring from the TTF unit to the butadiyne moiety. Although ^{13}C NMR chemical shifts are inherently insensitive to ring-current shielding effects, thus limiting the probe nuclei available across the all-carbon butadiyne chain to ascertain the position of the CBPQT[4+] ring in the oxidized state **1**[6+], a series of one-dimensional (1D) nuclear Overhauser effect (NOE) experiments (Figure 4) clearly showed the presence of through-space correlations between the resonances for the methylene protons neighboring the butadiyne units and those for the CBPQT[4+] ring in **1**[6+], interactions that were not present in **1**[4+]. Additionally, NOE correlations that were present between the signals for the methylene protons neighboring the TTF unit and

(22) Many dynamic processes exist for mechanically interlocked systems. Within CBPQT[4+]-based catenanes, the most common dynamic co-conformation and conformation processes include circumrotation of the CBPQT[4+] ring relative to the other macrocycle as well as phenylene and bipyridinium rotation within the CBPQT[4+] ring itself. Dynamic ^{1}H NMR experiments (Figure S7 in the Supporting Information) show dramatic changes upon varying the temperature, especially in the CBPQT[4+] resonances, as a consequence of these processes. For a recent review of the dynamics and stereochemistry of CBPQT[4+]-based [2]catenanes, see: Vignon, S. A.; Stoddart, J. F. *Collect. Czech. Chem. Commun.* **2005**, *70*, 1493–1576.

(23) Souizi, A.; Robert, A. *J. Org. Chem.* **1987**, *52*, 1610–1611.

(24) For a detailed description of this chemical oxidant and the reasons we used it here, see: (a) Tseng, H.-R.; Vignon, S. A.; Stoddart, J. F. *Angew. Chem., Int. Ed.* **2003**, *42*, 1491–1495. For a review of this and other chemical oxidants commonly used in NMR studies, see: (b) Connelly, N. G.; Geiger, W. E. *Chem. Rev.* **1996**, *96*, 877–910.

those for the CBPQT^{4+} ring in **1**$^{4+}$ disappeared after it was switched to **1**$^{6+}$. The resonances of the CBPQT^{4+} ring were shifted and also substantially simplified upon oxidation to **1**$^{6+}$. Both the α- and β-bipyridinium protons as well as the methylene protons within the cyclophane become homotopic, since they are no longer under the influence of the local symmetry of the TTF unit. This increased symmetry indicates that, not surprisingly, rotation of the cyclophane around the butadiyne unit is fast on the NMR time scale. Finally, the addition of 2 equiv of Zn dust to rereduce **1**$^{6+}$ restored the original spectrum of **1**$^{4+}$ (Figure 3c), indicating that the TTF unit once again resides within the CBPQT^{4+} cavity.

The switching of **1**·4PF$_6$ was also induced electrochemically. Cyclic voltammetry (CV) experiments (Figure 5) using NBu$_4$PF$_6$ as the electrolyte in MeCN were performed to probe the TTF-centered oxidation processes, specifically the reversible TTF → TTF$^{•+}$ and TTF$^{•+}$ → TTF^{2+} one-electron events. These processes are well-resolved in the cyclic voltammogram of compound **3** (Figure 5b), which displays two distinct oxidation peaks centered at +404 and +793 mV (vs Ag/AgCl), respectively. It has been well-established[5] that when TTF is encircled by the electron-poor CBPQT^{4+} ring, its first oxidation is shifted substantially to more positive potentials, usually close to the potential for the second oxidation for unencircled TTF. Thus, the first oxidative scan of **1**·4PF$_6$ (Figure 5a) shows only one broad peak

centered at 714 mV (vs Ag/AgCl) encompassing both of the distinct one-electron processes that together produce TTF^{2+} from the neutral TTF unit via TTF$^{•+}$. The translation of the CBPQT^{4+} ring is intimately involved with this oxidation process and is known[5] to occur upon the first oxidation to the TTF$^{•+}$ species, leaving the second oxidation to TTF^{2+} to occur at the same potential it would in the absence of the macrocycle. In the case of traditional multistation TTF-based catenanes or rotaxanes, such as [2]catenane **2**·4PF$_6$, the first oxidative scan contains signals attributed[5b,6g−i] to the first TTF oxidation at lower potentials for unencircled co-conformations. Indeed, integration of the first oxidation at lower potentials relative to the other oxidative signals forms the basis for determining the ratio of metastable to ground-state co-conformations within the molecular ensemble of these traditional multistation switches. No such first oxidative signal was present for **1**·4PF$_6$, indicating that there is only one available station for the CBPQT^{4+} ring: it encircles the TTF fully in the ground state, and no other translational states exist.

Performing two successive oxidative scans at various scan rates and temperatures allows the elucidation of the kinetics associated with the return of the CBPQT^{4+} ring from the oxidized co-conformation to the ground-state co-conformation (GSCC).[5b,6g−i] In traditional bistable MIMs, oxidation of the TTF unit in the first CV scan forces the CBPQT^{4+} ring onto
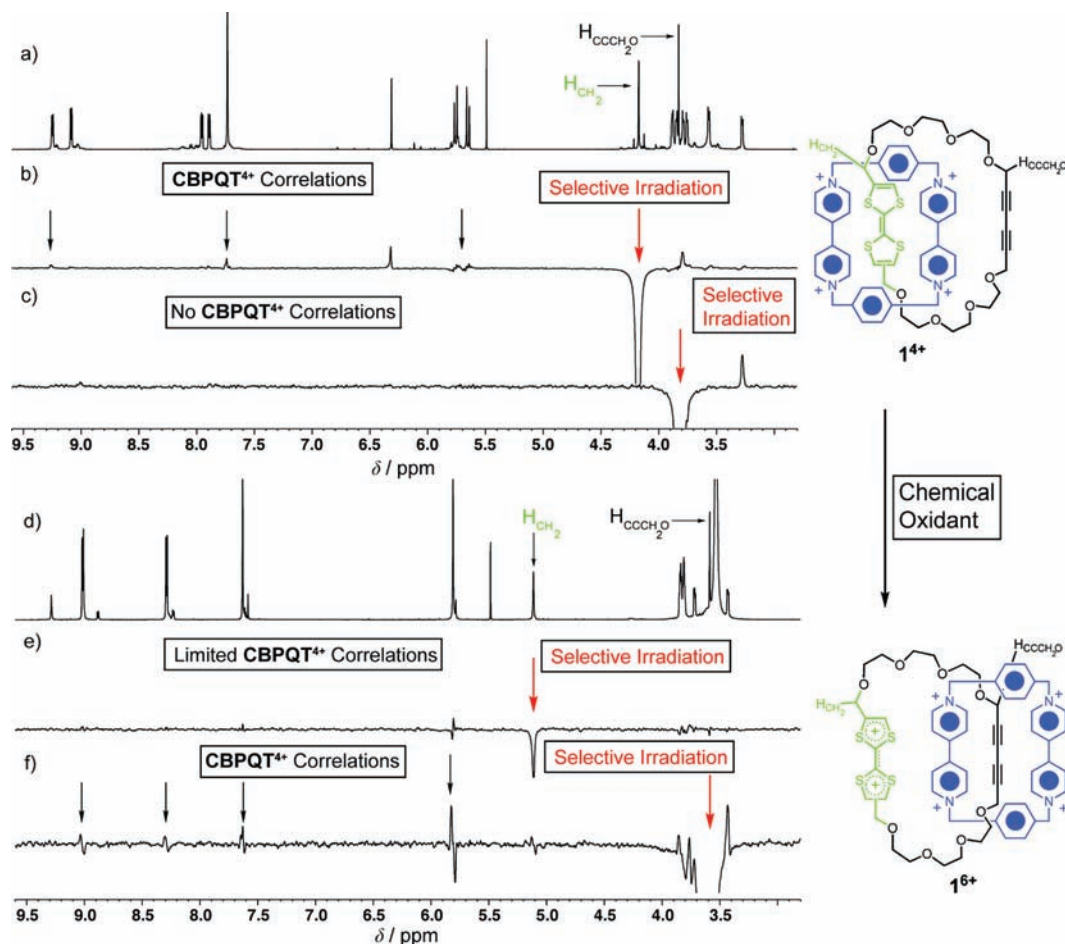

Figure 4. 1D NOE through-space correlations in **1**$^{4+}$ and **1**$^{6+}$ (600 MHz, 273 K). (a) ^{1}H NMR spectrum of **1**$^{4+}$, which displays (b) through-space correlations with the **CBPQT^{4+}** ring after selective pulsing of the H$_{CH_2}$ nearest the TTF moiety but (c) no through-space correlations with the **CBPQT^{4+}** ring after selective pulsing of the H$_{CCCH_2O}$ nearest the diyne. (d) ^{1}H NMR spectrum of **1**$^{6+}$, which (e) displays no through-space correlations with the **CBPQT^{4+}** ring after selective pulsing of the H$_{CH_2}$ nearest the TTF moiety but (f) does display through-space correlations with the **CBPQT^{4+}** ring after selective pulsing of the H$_{CCCH_2O}$ nearest the butadiyne. Additional 1D NOE correlations not highlighted with a black arrow are attributable to close interactions with the nearest-neighbor protons of the selectively irradiated resonances rather than through-space correlations between protons within each macrocycle of the catenane.

the weaker binding station. Because the CBPQT[4+] ring has an affinity for the weaker binding station (i.e., it sits in a local energy minimum), reduction of the TTF unit to its neutral state does not immediately result in a return to the GSCC. This co-conformation, in which the CBPQT[4+] ring encircles the weaker binding station while the TTF unit is in its neutral state, is known[5b] as the metastable-state co-conformation (MSCC). The conversion of the MSCC to the GSCC is an activated process, so it occurs over a finite time period (between the first and second successive CV scans) and depends[5] upon both the temperature and the environment of the MIM. However, no matter how high the scan rate or how low the temperature used in the CV experiments (1000 mV/s and 263 K, shown in Figure 5a), the presence of an MSCC, which would be indicated by the first oxidation of unencircled TTF in the second scan, was not observed[25] for **1**·4PF₆. In contrast to the case of single-station catenane **1**·4PF₆, a thorough electrochemical investigation of the MSCC-to-GSCC relaxation process for two-station catenane **2**·4PF₆ was possible[6g] across a range of scan rates and temperatures between 263–283 K because the weaker-binding DNP station slows the return of the CBPQT[4+] ring to the TTF unit. The lack of any observable MSCC for **1**·4PF₆ suggests that the butadiyne moiety has very little, if any, affinity for the tetracationic macrocycle and serves as no more than a passive bystander following a convenient catenation protocol for the formation of this [2]catenane, i.e., there is no experimental evidence for an electronic interaction, be it stabilizing or destabilizing, between the butadiyne moiety and the CBPQT[4+] ring.

Substantial changes occur in the UV–vis spectrum of **1**·4PF₆ upon electrochemical oxidation. The UV–vis spectrum of **1**⁴⁺

Figure 6. Spectroelectrochemistry (MeCN, 100 mM NBu₄PF₆) of (a) **1**⁴⁺, displaying a strong absorption centered at 830 nm corresponding to the TTF–CBPQT[4+] CT absorption, (b) **1**⁶⁺ after sustained current flow at +1.2 V, where the CT absorption is replaced by a strong absorption arising from TTF²⁺ at 400 nm, and (c) **1**⁴⁺ reformed after sustained reduction at 0 V, displaying the regained CT absorption.

in MeCN (with 100 mM NBu₄PF₆) (Figure 6a) contains a broad charge-transfer (CT) absorption centered at 830 nm, characteristic of a CBPQT[4+]-encircled TTF. The catenane was fully switched to **1**⁶⁺ after passage of a sustained current held at +1.2 V (vs Ag/AgCl) for several hours[26] in a custom-built spectroelectrochemical cell,[27] as indicated by the complete loss of the CT band at 830 nm and the appearance of a band at 400 nm characteristic of the TTF²⁺ dication. Interestingly, the lack of any transition that can be attributed to an electronic interaction
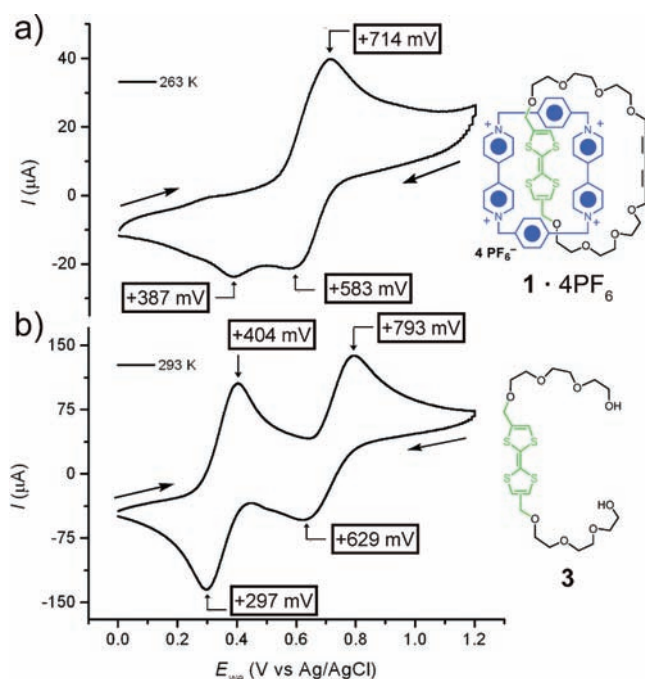

Figure 5. Oxidative cyclic voltammograms (second scans, MeCN, 100 mM NBu₄PF₆, 1000 mV/s) of (a) **1**·4PF₆, displaying the overlapping first and second oxidations of the TTF moiety to TTF²⁺ (performed at 263 K), and (b) **3**, displaying two distinct one-electron oxidation processes that give TTF•⁺ and then TTF²⁺ (performed at 298 K). The first and successive oxidative scans of **1**·4PF₆ were identical. For clarity, only the second oxidative scans are shown.
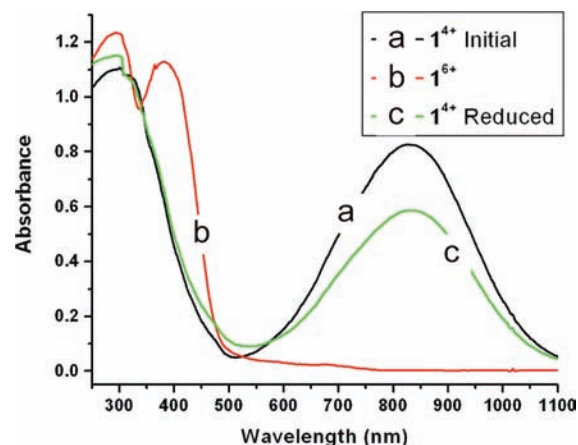
(25) The first-order decay from the MSCC, where the CBPQT[4+] ring encircles the butadiyne unit, to the GSCC, where the CBPQT[4+] ring encircles the TTF unit, can be fitted using the general formula given in eq 1:

$$N_{\text{butadiyne}}(t) = N^{\circ}_{\text{butadiyne}} + (N_{\text{total}} - N^{\circ}_{\text{butadiyne}}) \exp(-t/\tau) \quad (1)$$

where $N^{\circ}_{\text{butadiyne}}$ is the equilibrium population (0%) of the MSCC in the ground state at the beginning of the experiment, $N_{\text{butadiyne}}$ is the metastable-state population at the time t elapsed from the second reductive peak of the first scan to where the first oxidative peak for unencircled TTF would occur in the second successive scan, N_{total} is the total population of translational isomers, and τ is the lifetime of the metastable state. Solving eq 1 for $1/\tau$ yields the rate constant k for the relaxation process, which may be substituted into the variant of the Arrhenius equation given by eq 2,

$$k = \frac{k_{\text{B}}T}{h} \exp(-\Delta G^{\ddagger}/RT) \quad (2)$$

to yield $\Delta G^{\ddagger}$ for the relaxation process. For a detailed analysis, see ref 5b. A rigorous analysis could not be applied for **1**·4PF₆ because no metastable state could be observed. If it is assumed that a 1% population of the metastable state could be observed using a 1000 mV/s scan rate at 263 K (corresponding to $t = 0.8$ s for an ~800 mV peak separation), a k value of 2.9 s⁻¹ can be estimated from eq 1, which translates into a minimum experimentally measurable $\Delta G^{\ddagger}$ of 14.8 ± 1 kcal/mol for the MSCC-to-GSCC relaxation process.
(26) As opposed to CV, spectroelectrochemistry relies on the complete oxidation or reduction of the analyte across the entire path length of the cell. The long waiting times are therefore not a reflection of the kinetics of switching a single molecule but of the diffusion of molecules to and from the working electrode.
(27) The cell is an optically transparent thin-layer electrochemical (OTTLE) cell with an optical path of 1 mm that uses a Pt grid as the working electrode, a Pt wire as the counter electrode, and a Ag/AgCl reference electrode. For the construction of this cell, see: Babaei, A.; Connor, P. A.; McQuillan, A. J.; Umapathy, S. *J. Chem. Educ.* **1997**, *74*, 1200–1204.
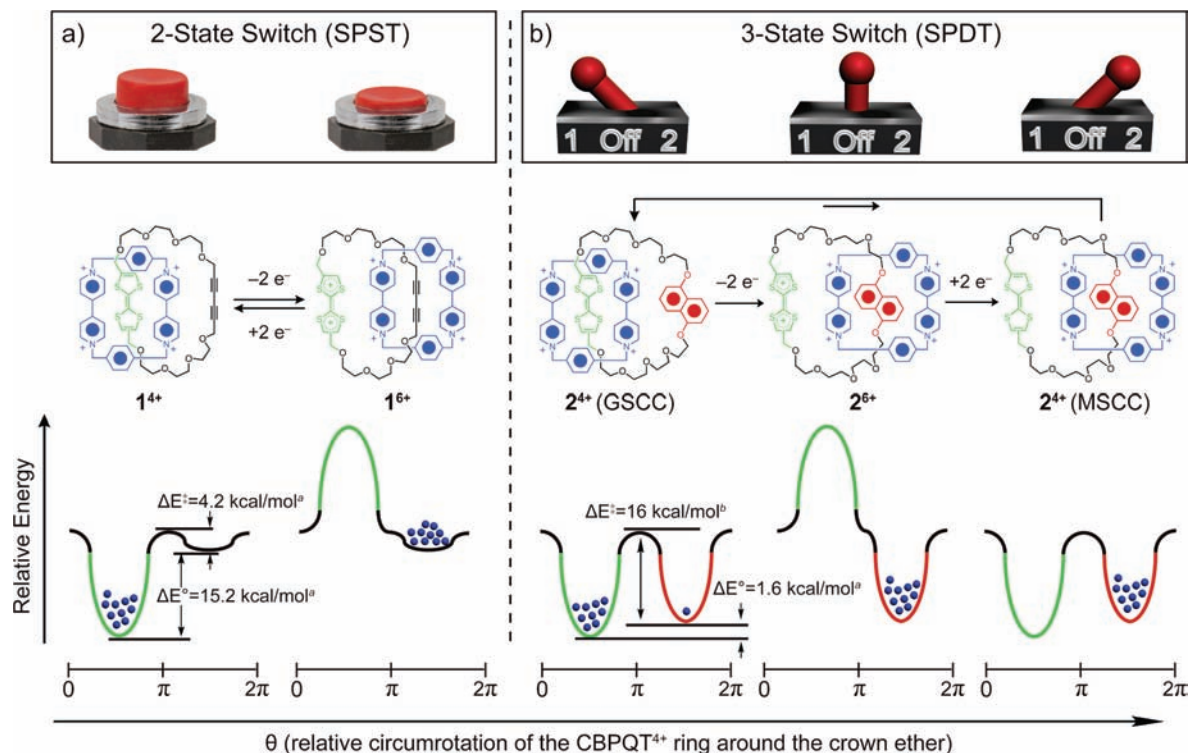
Figure 7. Relative energy surface diagrams depicting the energetic consequences of electrochemically switching the TTF to TTF^{2+} in (a) the single-station catenane **1**·4PF$_6$ and (b) the traditional double-station catenane **2**·PF$_6$; the CBPQT^{4+} ring position in each case is represented by blue spheres. Compound **1**$^{4+}$ exists as a single translational state that may be switched wholly to its inverse state as described by a 180° circumrotation of the CBPQT^{4+} ring around the TTF-containing crown ether to arrive at **1**$^{6+}$, where the CBPQT^{4+} ring sits in a local minimum only as a consequence of its aversion to the TTF^{2+} dication. Conversely, **2**$^{4+}$ exists as a mixture of the GSCC and MSCC, in which the CBPQT^{4+} ring encircles the TTF and DNP units, respectively. Upon oxidation of the TTF unit, the CBPQT^{4+} ring encircles only the DNP unit of **2**$^{6+}$ and remains there for a finite length of time even after reduction of the TTF unit to re-form **2**$^{4+}$. Values labeled with "a" superscripts were calculated as described in the text; the one labeled with the "b" superscript was measured and originally reported in ref 6g.

between the butadiyne moiety and the CBPQT^{4+} ring in **1**$^{6+}$ (Figure 6b) supports the hypothesis that there is no affinity between these two components. The original (albeit somewhat attenuated[28]) spectrum of **1**$^{4+}$ was restored after rereduction (Figure 6c) by holding the potential at 0 V (vs Ag/AgCl) for several hours.

The experimental data illustrate a generalized view of the changes in the energy surface of **1**·4PF$_6$ upon electrochemical switching (Figure 7). In order to investigate the exact nature of this energy landscape, we turned to quantum-mechanical modeling. Because only one translational state was observed for **1**·4PF$_6$ in the first scan using CV, the energy of the co-conformation in which the CBPQT^{4+} ring encircles the butadiyne unit relative to that with the TTF unit encircled could not be directly measured. Equally challenging was the fact that the rate of return of the CBPQT^{4+} ring to the TTF unit after restoration of the ground state of the oxidized catenane occurs far too quickly to measure, thus preventing the experimental calculation of the barrier to circumrotation of the CBPQT^{4+} ring around the crown ether. In any event, quantum-mechanical investigations provided the means to study these key processes in more detail on the extremely short time scales at which the molecular switch **1**·4PF$_6$ operates.

In order to understand the energy profile and mechanism of the switching process for **1**$^{4+}$, we turned to density functional

theory (DFT) of the M06 variety,[29] which we have shown[30] to be a good choice for the study of similar rotaxane-based architectures. We performed geometry optimizations for the TTF-encircled (GSCC) and butadiyne-encircled (MSCC) translational isomers of **1**$^{4+}$ at the M06/6-31G** level of theory, leading to the predicted structures displayed in Figure 8. We calculated a difference of 15.2 kcal/mol between the binding energies of the GSCC and MSCC in MeCN solvent. This predicted energy difference between the GSCC and MSCC suggests a GSCC/MSCC population ratio of 10^{11}:1 at 298 K.

Since we were most interested in learning about the energy profile for the switching process, we mapped the potential energy surface by performing a manually steered scan of the rotation of the TTF−butadiyne macrocycle with respect to the electron-deficient CBPQT^{4+} ring. We used the less computationally expensive M06-L functional to generate structures along the path from the MSCC to the GSCC. After further optimization of the highest-energy structures (using the M06 functional), we estimate that the process of resetting the MSCC to the GSCC has a barrier of ~4.2 kcal/mol. These results agree with the inability to observe an MSCC under the experimental conditions employed (263 K, 1000 mV/s).[27] Our estimated barrier of ~4.2 kcal/mol for resetting the MSCC to the GSCC corresponds to a 2 × 10^{-10} s (~200 ps) relaxation time at 298 K (~600 ps at

(28) The attenuation in signal intensity (Figure 6) is attributed to electrochemical destruction of the molecule over the course of the investigation.

(29) Zhao, Y.; Truhlar, D. G. *Theor. Chem. Acc.* **2008**, *120*, 215–241. (b) Zhao, Y.; Truhlar, D. G. *Acc. Chem. Res.* **2008**, *41*, 157–167.
(30) Benítez, D.; Tkatchouk, E.; Yoon, I.; Stoddart, J. F.; Goddard, W. A., III. *J. Am. Chem. Soc.* **2008**, *130*, 14928–14929.

263 K). Although this small "barrier" to circumrotation may be partly due to weak binding between the butadiyne fragment and the CBPQT^{4+} ring (the HOMO-1−LUMO interaction), it is most likely dominated by the accompanying stabilizing interaction with the HOMO, which is located almost entirely on the neutral TTF unit.[31] Figure 8c depicts the empty orbital on the CBPQT^{4+} cyclophane (the LUMO, shown in red and blue) and the doubly occupied orbitals on the TTF unit (the HOMO, in green and turquoise) and the butadiyne fragment (the HOMO-1, in brown and gold). From these calculations, we can estimate the excitation energy for a possible CT
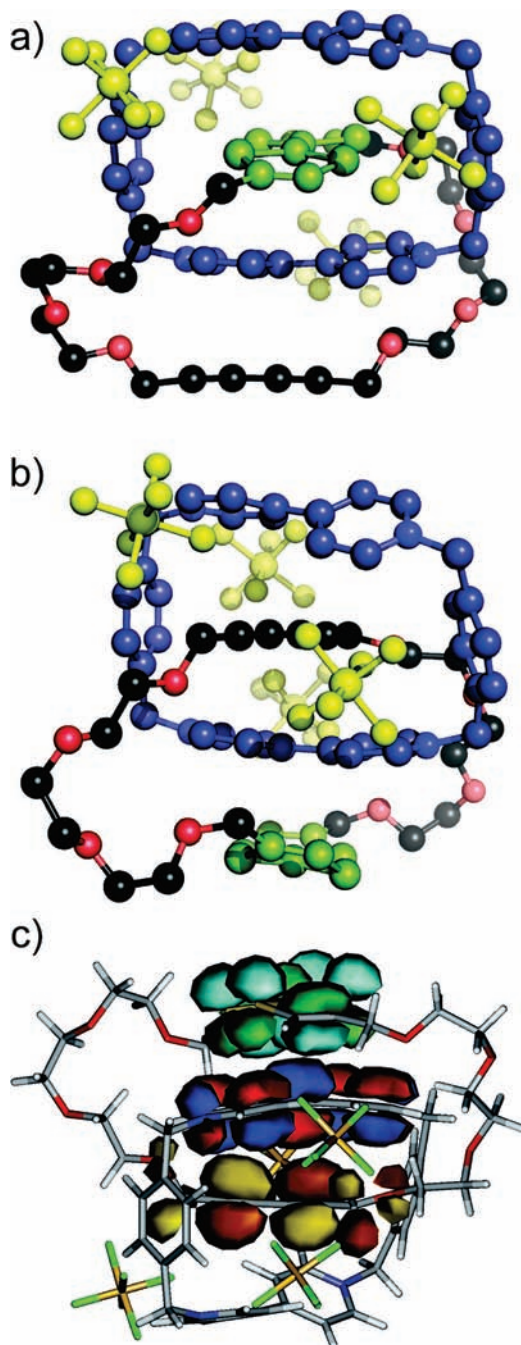

Figure 8. Computed structures for **1**$^{4+}$ in (a) the ground-state coconformation (GSCC) and (b) metastable-state coconformation (MSCC). (c) The MSCC for **1**$^{4+}$ has the LUMO (depicted in red and blue) localized on the CBPQT^{4+} ring, whereas the HOMO (depicted in green and turquoise) is localized on the TTF unit and the HOMO-1 (depicted in brown and gold) on the butadiyne unit.

transition between the CBPQT^{4+} ring and the encircled butadiyne moiety for the oxidized translational state **1**$^{6+}$. Using the experimental value for the CBPQT^{4+}-encircled TTF CT absorption band (λ_{max} = 830 nm; Figure 6) and the calculated HOMO (−0.1957 au) and HOMO-1 (−0.2477 au) energies yields an estimated LUMO energy of +0.1415 au. If it is assumed that these relative energies apply to the oxidized catenane **1**$^{6+}$, a CT transition between the **1**$^{6+}$ HOMO (the HOMO-1 in **1**$^{4+}$) localized on the butadiyne unit and the **1**$^{6+}$ LUMO+1 (the LUMO in **1**$^{4+}$) would lead to an absorption[32] centered around ∼425 nm, which would likely overlap and be eclipsed by the intense absorption of the TTF^{2+} dication.

Our experimental and computational results strongly suggest that the catenane **1**·4PF$_6$ behaves as a very simple push-button molecular switch (Figure 7a) in which the ground state contains two local minima having vastly different energies (separated by 15.2 kcal/mol), ensuring that the TTF-encircled translational state is nearly solely populated (roughly 1 out of every ∼10^{11} molecules exists in the other translational state). Oxidation of the TTF unit (i.e., "pushing the button") inverts the local minimum into a local maximum, thereby effecting the circumrotation of the CBPQT^{4+} ring around its companion macrocycle to the local minimum on the butadiyne moiety, where it rests securely as long as the TTF^{2+} moiety retains its dicationic character. Inversion of the local maximum around the TTF^{2+} dication by reduction to the neutral species (i.e., "releasing the button") re-establishes the situation represented by the original energy diagram, causing the CBPQT^{4+} ring to migrate quickly (in several hundred picoseconds) over a very small "barrier" (estimated to be $\Delta E^{\ddagger} \approx$ 4.2 kcal/mol) and reoccupy the deep well it enjoys by encircling the TTF unit. This very small $\Delta E^{\ddagger}$ value, although technically an activation barrier, hardly constitutes even what we might call a "speed bump" for the circumrotation, so the process occurs at the "diffusion"-controlled rate of 5 × 10^9 s^{-1} at room temperature, allowing the mechanical switching from **1**$^{6+}$ to **1**$^{4+}$ to occur almost instantaneously.

This situation is quite different from that for the traditional two-station [2]catenane **2**·4PF$_6$ (Figure 7b), in which a battle is waged between the TTF and DNP units for occupancy by the CBPQT^{4+} ring in the ground state, until the establishment of an equilibrium characterized by an ensemble in which the CBPQT^{4+} ring occupies the TTF and DNP local energy minima in a 9:1 ratio based on the $\Delta G°$ value of 1.6 kcal/mol.[5b] In this case, oxidation of the TTF unit converts its position from a local minimum to a local maximum, making the DNP unit the sole local minimum and causing all of the CBPQT^{4+} rings to migrate and encircle it. Although rereduction of the TTF^{2+} dication reestablishes the TTF unit as the global minimum, the CBPQT^{4+} rings remain kinetically trapped within the DNP local energy well for some time, until they transverse a relatively large barrier ($\Delta G^{\ddagger}$) of 16 kcal/mol[33] in order to equilibrate once again and form the 9:1 ratio of co-conformers. While a complex interplay

(31) Our calculations did not include entropic corrections, which could lower the energy for the MSCC and the circumrotation barrier by 2−4 kcal mol^{-1} as a consequence of the greater vibrational freedom of the butadiyne and the oligomeric ethylene glycol chain inside the CBPQT^{4+} ring.

(32) This somewhat crude estimate of the proposed electronic transition between the butadiyne and CBPQT^{4+} ring in **1**$^{6+}$ is based upon energy levels calculated without applying a solvent correction for **1**$^{4+}$, and while there would be some variation in the energies as a consequence of the added charge, we speculate that the error in the calculation would amount to no more than 40 nm.

(33) Originally reported in ref 6g.

between local energy minima and transient excited states allows the switching within the two-station catenane **2**·4PF$_6$, the situation is much less complicated in the case of the single-station catenane **1**·4PF$_6$, where the simple "push of a button" toggles between two energy surfaces, each having a singly occupied minimum.

Conclusion

We have demonstrated the efficient synthesis of, for all intents and purposes, a single-station yet switchable hetero[2]catenane by means of the Eglinton coupling-based macrocyclization of a TTF thread around a CBPQT^{4+} ring. The simplicity of the synthetic approach and molecular design belie the effectiveness of **1**·4PF$_6$ as a perfect switch in which the ensemble is nearly completely composed of distinct single co-conformations in the ground and excited states. The push-button-switching nature of **1**·4PF$_6$ sheds light upon the operation of switchable mechanically interlocked molecules, tempting us to celebrate the simplicity of a switchable single-station architecture in the context of more complicated (and synthetically more challenging) molecular targets. The unique combination of two discrete translational forms, coupled with the ability to toggle completely between these two electrochemically controllable states, positions this push-button molecular switch as an ideal candidate for introduction into solid-state electronic device settings. It is toward these and other goals that we will continue to apply mechanically interlocked architectures afforded by Eglinton coupling and other mild alkyne-based reactions.

Experimental Methods

General Methods. All of the reagents were purchased from commercial suppliers (Aldrich or Fisher) and used without further purification. Cyclobis(paraquat-*p*-phenylene) hexafluorophosphate,[7b] 1-iodo-8-tetrahydropyranyloxy-3,6-dioxaoctane,[34] and 4,4′(5′)-bis-(methanol)tetrathiafulvalene[35] were prepared according to literature procedures. Thin-layer chromatography (TLC) was performed on silica gel 60 F$_{254}$ (E. Merck). Column chromatography was performed on silica gel 60F (Merck 9385, 0.040−0.063 nm). NMR spectra were recorded at 25 °C (unless otherwise noted) on Bruker Avance 500 and 600 spectrometers with working frequencies of 500 and 600 MHz for ^{1}H nuclei and 125 and 150 MHz for ^{13}C nuclei, respectively. Chemical shifts are reported in parts per million relative to the signals corresponding to the residual nondeuterated solvents.[36] All of the ^{13}C spectra were recorded with simultaneous decoupling of proton nuclei. Transient ^{1}H−^{1}H NOE experiments were performed using a double-pulsed field-gradient spin−echo NOE (DPFGSE-NOE) pulse sequence with a mixing time of 600 ms. Electrospray ionization (ESI) mass spectrometry (MS) was performed using an Agilent 6210 LC-TOF high-resolution (HR) mass spectrometer. CV experiments were performed on a Princeton Applied Research 263 A multipurpose instrument interfaced to a PC using a glassy carbon working electrode (0.018 cm^2, Cypress Systems). The electrode surface was polished routinely with a 0.05 μm^2 alumina/water slurry on a felt surface immediately before use. The counter electrode was a Pt coil, and the reference electrode was a AgCl-coated Ag wire. The concentrations of the samples

were 1 mM in 100 mM electrolyte solution (NBu$_4$PF$_6$ in MeCN). UV−vis absorption spectra were recorded on a Varian Cary 300 spectrophotometer. X-ray intensity data were measured on a Bruker APEX II CCD system equipped with a graphite monochromator and a Cu Kα ImuS microsource (λ = 1.54178 Å).

Computational Methods. Calculations were performed on all of the systems using DFT with the M06-L or M06 functional, as implemented in Jaguar 7.6.[37] The M06 functional is a new hybrid metageneralized-gradient-approximation exchange-correlation functional that leads to impressive accuracy for a very large validation set of systems, including van der Waals dimers, reactions, and transition-metal complexes. Starting with a structure from crystallographic data, we optimized the geometry using the 6-31G** basis set with the M06 functional in the gas phase. Single-point energies were calculated using the M06 functional and the 6-311++G** basis set. Solvent corrections were based on single-point self-consistent Poisson−Boltzmann continuum-solvation calculations for acetonitrile (ε = 37.5, R_0 = 2.18 Å) using the PBF module in Jaguar.

Preparation of 3. 4,4′(5′)-Bis(methanol)tetrathiafulvalene (1.500 g, 5.673 mmol) was added to a slurry of NaH (60% dispersion in oil, 1.743 g, 43.57 mmol) in dry THF (700 mL), and the mixture was heated under reflux under an N$_2$ atmosphere for 1 h. A solution of 1-iodo-8-tetrahydropyranyloxy-3,6-dioxaoctane (7.420 g, 21.56 mmol) in dry THF (75 mL) was added to the reaction mixture dropwise over 1 h. The reaction mixture was refluxed under an N$_2$ atmosphere for 24 h. After the mixture was cooled to room temperature (rt) and MeOH was added, the solution was filtered through a plug of silica, and the solvents were removed in vacuo. The crude brown oil was partitioned between CH$_2$Cl$_2$ (300 mL) and 1 M NH$_4$Cl (300 mL), the organic phase washed with H$_2$O (1 × 100 mL) and brine (1 × 100 mL) and then dried (MgSO$_4$), and the solvent removed in vacuo. The residual brown oil was dissolved in a 1:1 CH$_2$Cl$_2$/MeOH mixture (150 mL), and HCl (0.4 mL, 12 M) was added. The solution was stirred at rt for 1.5 h, after which 1 M NaOH (200 mL) was added. The mixture was extracted with CH$_2$Cl$_2$ (3 × 100 mL) and dried (MgSO$_4$), and the solvent was removed in vacuo. The resulting material was subjected to chromatography (SiO$_2$, 97:3 to 95:5 CH$_2$Cl$_2$/MeOH eluent) to provide a yellow oil (1.316 g, 44%). Data for **3**: ^{1}H NMR (500 MHz, CD$_2$Cl$_2$): δ 6.27 (s, 2H, SC*H*), 4.26 (s, 4H, SCC*H*$_2$), 3.68−3.54 (m, 24H), 2.59−2.49 (m, 2H, O*H*). ^{13}C NMR (125 MHz, CD$_2$Cl$_2$): δ 135.04, 134.94, 116.87, 116.75, 110.82, 72.91, 72.89, 70.99, 70.80, 70.70, 69.78, 69.77, 68.50, 62.02. HRMS (ESI) *m/z*: Calcd for C$_{20}$H$_{32}$O$_8$S$_4$: 528.0980. Found: 529.1046 ([M + H]$^+$).

Preparation of 4. A solution of propargyl bromide in PhMe (80% by weight, 0.930 mL, 10.4 mmol) was added to a mixture of **3** (920 mg, 1.74 mmol) and NaOH (696 mg, 17.4 mmol) in THF (20 mL). The mixture was heated at 60 °C under ambient atmosphere for 24 h. The mixture was partitioned between EtOAc (100 mL) and 1 M NH$_4$Cl (100 mL), and the aqueous phase was washed with EtOAc (2 × 75 mL). The combined organic phases were washed with 1 M NH$_4$Cl (75 mL) and brine (75 mL) and dried (MgSO$_4$), and the solvent removed in vacuo. The resulting material was subjected to chromatography (SiO$_2$, 1:1 to 8:3 EtOAc/hexanes eluent) to provide a brown oil (704 mg, 67%). Data for **4**: ^{1}H NMR (500 MHz, CD$_2$Cl$_2$): δ 6.26 (s, 2H, SC*H*), 4.27 (s, 4H, SCC*H*$_2$), 4.17 (d, $^4J_{HH}$ = 2.3 Hz, 4H, C≡CC*H*$_2$O), 3.66−3.58 (m, 24H), 2.49 (t, $^4J_{HH}$ = 2.3 Hz, 2H, C≡C*H*). ^{13}C NMR (125 MHz, CD$_2$Cl$_2$): δ 135.06, 135.00, 116.81, 116.71, 80.23, 74.65, 70.94, 70.90, 70.85, 70.70, 69.78, 69.60, 68.47, 58.63. HRMS (ESI) *m/z*: Calcd for C$_{26}$H$_{36}$O$_8$S$_4$: 604.1293. Found: 604.1310 (M$^+$), 622.1634 ([M + NH$_4$]$^+$), 627.1191 ([M + Na]$^+$).

Preparation of 1·4PF$_6$. Cu(OAc)$_2$·H$_2$O (61.4 mg, 0.295 mmol) was added to a green solution of **4** (71.2 mg, 0.118 mmol) and CBPQT·4PF$_6$ (65.0 mg, 0.059 mmol) dissolved in MeCN (45 mL), and the solution was stirred for 48 h under ambient conditions.

(34) Fuchter, M. J.; Beall, L. S.; Baum, S. M.; Montalban, A. G.; Sakellariou, E. G.; Mani, N. S.; Miller, T.; Vesper, B. J.; White, A. J. P.; Williams, D. J.; Barrett, A. G. M.; Hoffman, B. M. *Tetrahedron* **2005**, *61*, 6115−6130.

(35) Andreu, R.; Garín, J.; Orduna, J.; Savirón, M.; Cousseau, J.; Gorgues, A.; Morisson, V.; Nozdryn, T.; Becher, J.; Clausen, R. P.; Bryce, M. R.; Skabara, P. J.; Dehaen, W. *Tetrahedron Lett.* **1994**, *35*, 9243−9246.

(36) Gottlieb, H. G.; Kotlyar, V.; Nudelman, A. *J. Org. Chem.* **1997**, *62*, 7512−7515.

(37) *Jaguar*, version 7.0; Schrödinger, LLC: New York, 2007.

The solvent was removed in vacuo, and the green residue was subjected to chromatography (SiO$_2$, Me$_2$CO to 1% NH$_4$PF$_6$ in Me$_2$CO eluent). The green band was collected, concentrated in vacuo, and treated with cold H$_2$O to precipitate a green solid (64.4 mg, 64%). Data for **1**·4PF$_6$: ^{1}H NMR (600 MHz, CD$_3$CN, 0 °C): δ 9.15 (d, $^3J_{HH}$ = 6.7 Hz, 4H, α-CBPQT^{4+}-*H*), 8.99 (d, $^3J_{HH}$ = 6.7 Hz, 4H, α-CBPQT^{4+}-*H*), 7.89−7.87 (m, 4H, β-CBPQT^{4+}-*H*), 7.83−7.81 (m, 4H, β-CBPQT^{4+}-*H*), 7.66 (s, 8H, *p*-xylyl CBPQT^{4+}), 6.26 (s, 2H, SC*H*), 5.73−5.59 (m, 8H, CBPQT C*H*$_2$), 4.15 (s, 4H, SCC*H*$_2$), 3.87−3.86 (m, 4H), 3.84−3.82 (m, 4H), 3.81 (s, 4H, C≡CC*H*$_2$O), 3.78−3.76 (m, 4H), 3.75−3.73 (m, 4H), 3.57−3.54 (m, 4H), 3.28−3.26 (m, 4H). ^{13}C NMR (125 MHz, CD$_3$CN): δ 146.66, 145.69, 144.83, 136.94, 133.94, 131.73, 126.65, 126.23, 126.14, 120.30, 108.87, 76.93, 72.12, 71.56, 71.26, 71.21, 71.00, 70.76, 69.86, 68.83, 65.40, 59.15. HRMS (ESI) *m/z*: Calcd for C$_{62}$H$_{66}$F$_{24}$N$_4$O$_8$P$_4$S$_4$: 1702.2309 (M + 4PF$_6$), 1557.2669 ([M + 3PF$_6$]$^+$), 706.1514 ([M + 2PF$_6$]$^{2+}$), 422.4463 ([M + PF$_6$]$^{4+}$), 280.5937 (M^{4+}). Found: 1557.2734 ([M + 3PF$_6$]$^+$), 706.1514 ([M + 2PF$_6$]$^{2+}$). Mp: 155−158 °C (dec).

Supporting Information Available: Spectral characterization of all new compounds, VT and 2D ^{1}H NMR spectral data and reductive CV electrochemical data for **1**·4PF$_6$, and crystallographic data (CIF) for **1**·4PF$_6$. This material is available free of charge via the Internet at http://pubs.acs.org.

JA904104C